The effect of an adverse pressure gradient on the drag reduction performance of manipulators

A. M. Savill
Department of Engineering, University of Cambridge, Cambridge CB2 1PZ, UK

This paper presents skin friction data obtained with sublayer-scale fence, razor blade, and log-layer-sized Preston tube for both natural and manipulated boundary layers subjected to a strong adverse pressure gradient. Comparative measurements were made, under nominally zero pressure gradient conditions, with a floating element drag balance. The results provide support for established calibration formulas and recently proposed corrections for dp/dx and d^2p/dx^2. They also reveal that the adverse pressure gradient had remarkably little effect on the magnitude of the C_f reduction obtained by introducing an optimized tandem plate manipulator into the outer part of the boundary layer (to the extent that separation occurred when the manipulator was present). This finding is assessed in the light of other recent results and earlier floating element measurements. In addition, the skin friction distributions measured in the experiment are shown to be predicted remarkably accurately with an algebraic stress model. However, the computational results indicate an associated increase in the shape factor which probably limits any net benefit even prior to the onset of separation.

Keywords: boundary layer; manpulators; drag reduction; adverse pressure gradients; turbulence modeling

Introduction

An intensive effort by many research groups worldwide has established that turbulent skin friction can be reduced significantly by introducing very thin flat plate manipulators into the outer region of turbulent boundary layers. It would also appear that net drag reduction may be achieved with such outer layer devices, at least at sufficiently high chord Reynolds numbers under controlled laboratory conditions, provided these are carefully machined, set up, and tensioned to avoid vibration. Parametric drag measurements[1–7] have indicated the optimum configurational parameters required to achieve such reductions and, following detailed hot-wire and flow visualization surveys, some agreement has been reached regarding the possible mechanisms responsible for these.[8–12] More recently the existence, and to an extent the magnitude, of the optimum parameters for the preferred tandem arrangement (see Figure 1) have related to the maximization of specific drag reduction mechanisms.[12,13] However, such studies have provided only a partial explanation for the difference between the magnitude of the net reduction obtained in the most beneficial experiments ($<25\%$[14]) compared to those measured in other cases ($<8\%$[2,5,15,16]).

Attention is now being directed to practical aerodynamic applications for which such thin plate manipulators must necessarily be replaced by stronger, self-supporting, aerofoil section devices. Low-speed laboratory experiments[17,18] have shown that equivalent C_f reductions, and up to 7% net drag reduction, can be achieved using tandem NACA 0009 profile manipulators with essentially the same optimum parameters. The results of initial flight tests[19,20] have indicated that equivalent skin friction reductions can be achieved with similarly scaled, profiled manipulators at high Mach and Reynolds numbers. Some information is also available regarding other practical considerations, such as the effect of adverse pressure gradient,[2,14,21,22] free stream turbulence,[23] and rough[24,25] or Riblet[26,27] surfaces on manipulator performance. All three effects may be important in any application to the internal passages of aeroengines, and the first is particularly relevant to proposed external aircraft applications. However, previous pressure gradient studies have been restricted to weak laboratory gradients with $\beta<0.03$[14,15] or $\Delta p<0.006$ (Nguyen, private communication), except for some uncorrected Preston tube data at $\beta=0.2$[2,21] and 0.5,[20] and the flight test results with $\beta=0.2$–0.4 which were limited by experimental measurement difficulties and to an extent contaminated by three-dimensional effects. The present experiment was therefore intended to provide a more accurate assessment of the effect of a severe adverse pressure gradient on the drag-reducing performance of a tandem manipulator optimized for nominally zero pressure gradient conditions. In particular, the aim was to investigate how the imposition of such additional straining downstream of the device would influence the subsequent development of the manipulated boundary layer.

At the same time an attempt was made to predict the response

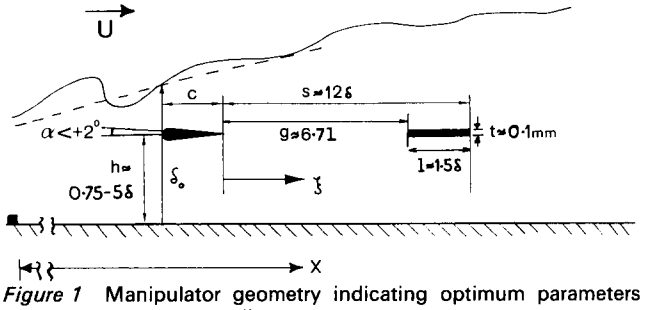

Figure 1 Manipulator geometry indicating optimum parameters derived from low Re studies

Address reprint requests to Dr. Savill at the Department of Engineering, University of Cambridge, Cambridge CB2 1PZ, UK.

Received 4 March 1988; accepted for publication 26 September 1988

of the boundary layer to such disturbances using an algebraic stress model (ASM) approximation to the turbulent transport equations. In view of the need to assess the performance of manipulators in boundary layers subjected to combinations of additional disturbances, particularly at high Reynolds numbers, there is a strong case for applying turbulence models to manipulated flows. From a modeling standpoint such flows are of inherent interest because they represent a step up in complexity from the boundary layers subjected to additional straining which were considered at the 1980–81 AFOSR-HTTM-Stanford conference on complex turbulent flows. The ASM scheme of Launder *et al.*[28] performed generally at least as well as higher-order Reynolds stress closures and considerably better than k-ε models on the simpler Stanford adverse pressure gradient test cases to which it was applied. The same model with essentially the same set of "standard" constants has subsequently been found to perform remarkably well on a range of confluent wake/boundary layer interactions in both zero[29] and adverse[30] pressure gradients. This model was therefore selected for initial attempts at modeling manipulated boundary layers with this level of closure, and again good results were achieved.[12,21] Further predictions for the adverse pressure gradient case are presented here.

Experiment

This was conducted in a blower tunnel of 1.5×0.3 m cross section with a 3-m long working section previously used for similar studies of wake/boundary layer interactions.[30] The boundary layer was tripped with a trip wire 0.8 m upstream of the position where the 0.8-m span tandem manipulator was located. The pressure gradient was imposed by altering the porosity of the roof and introducing a gauze resistance downstream. In this manner, as indicated by Figure 2, it was possible to maintain the pressure gradient close to zero in the vicinity of the tandem manipulator: $l = 1.5\delta$, $s = 10\delta$, $h = 0.75\delta$, and $t = 1$ mm. The free stream velocity at the first measurement station was $U = 13$ m/s, giving $\mathrm{Re}_\theta = 2700$ at the leading edge of the first plate, where the boundary layer thickness $\delta = 14$ mm, and $\mathrm{Re}_1 = 26{,}000$.

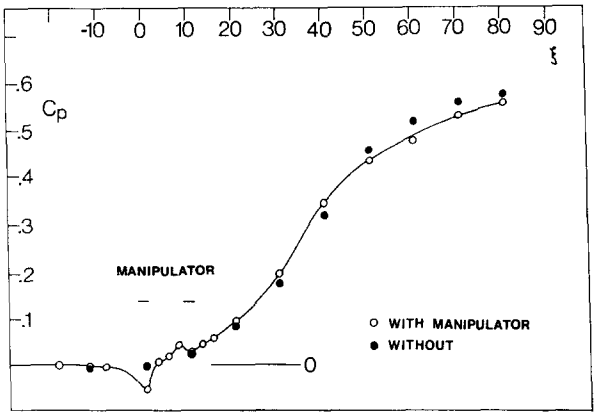

Figure 2 Imposed pressure gradient with and without manipulator

In Figure 3 the wall static pressure perturbation due to the device, obtained by differencing the two curves in Figure 2, is compared with that predicted by an inviscid computation as well as experimental measurements for similar drag single flat plate and aerofoil manipulators.[7,17,31,32] The present results confirm the conclusion of Bandyopadhyay and Watson[31] that a gap of approximately five chords is sufficient to isolate the individual pressure fields of the two elements of the tandem, while the close agreement with the nominally zero pressure gradient results indicates that the initial interaction between the flow and the manipulator was not altered by the weak gradient at the device location.

Downstream of the device the pressure gradient steepened rapidly with the pressure gradient parameter β reaching a maximum value of approximately 0.5 between the trailing edge of the second plate and $\xi = 60$. At the same time Δp reached a maximum of 0.015–0.02 for which Patel's analysis[33] suggests that preliminary measurements of C_f with the same logarithmic-layer-scale ($d^+ < 60$) Preston tube[21] could have been in error by more than 6%. The results presented in Figure 4 and Table 1 have therefore been corrected for the effects of $\mathrm{d}p/\mathrm{d}x$ using

Notation

c	Chord length of aerofoil manipulators
C_f	Local skin friction coefficient
C_p	Wall static pressure coefficient
d	Preston tube diameter
g	Gap between tandem manipulator plates
h	Height of manipulator above wall
h_{RB}	Height of razor blade edge above wall
h_F	Height of skin friction fence
H	Shape factor, θ/δ^*
k	Turbulence energy
l	Length of manipulator plates
p	Static pressure
q	Dynamic pressure
Re_1	Chord Reynolds number of manipulator
Re_θ	Momentum thickness Reynolds number
s	Spacing (leading edge to leading edge) of tandem manipulators
t	Thickness of manipulator plates
u	Turbulent velocity fluctuation
u_τ	Friction velocity
U	Free stream velocity
x	Coordinate in stream direction
y	Coordinate normal to wall boundary
z	Coordinate in spanwise direction
α	Angle of attack
β	Pressure gradient parameter, $(\theta/\tau)(\mathrm{d}p/\mathrm{d}x)$
Δp	Pressure gradient parameter, $(\nu/\rho u_\tau^3)(\mathrm{d}p/\mathrm{d}x)$
δ	Boundary layer thickness (to $U = 0.995U_0$)
δ^*	Displacement thickness
ε	Turbulent energy dissipation
ρ	Density
θ	Momentum thickness
τ	Wall shear stress
ν	Kinematic viscosity
ξ	Distance downstream of manipulator measured in terms of δ at its leading edge

Superscripts

+	Denotes wall units, $\times u_\tau/\nu$

Subscripts

0	Denotes value at the station in the natural boundary layer corresponding to the leading edge of the manipulator

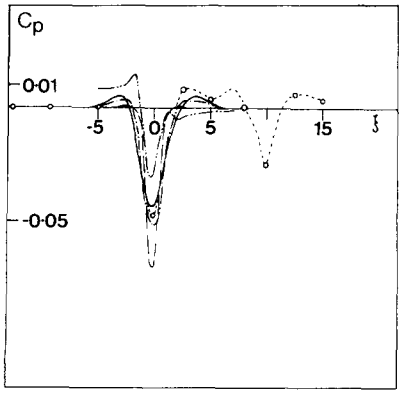

Figure 3 Wall static pressure distributions beneath single and tandem manipulators: – – ○ – –, present tandem results; single plates: —·—, $l=0.75\delta$, $h=0.3\delta$, $t=0.1$ mm, $Re_\theta=2500$, $Re_1=17{,}000$;[32] single NACA 0009 aerofoils: ——, $l=1.0\delta$, $h=0.8\delta$, $\alpha=0$, $Re_\theta=3300$, $Re_0=35{,}000$;[17] ——, $l=1.1\delta$, $h=0.88\delta$, $\alpha=0$, $Re_\theta=2700$, $Re_1=31{,}000$, ·—·, theory[31]

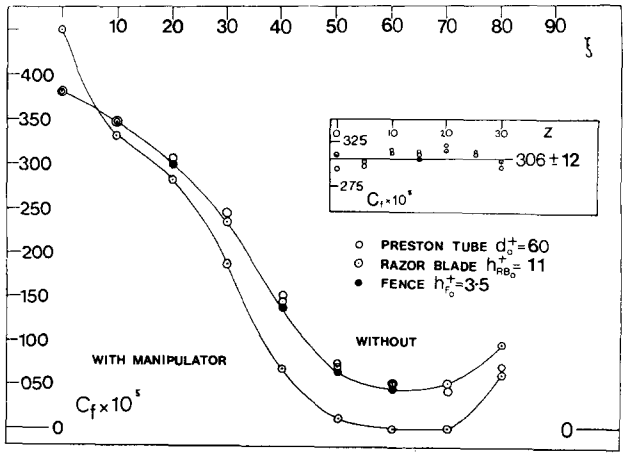

Figure 4 Skin friction measurements for natural and manipulated boundary layers subjected to severe adverse pressure gradient

Table 1 C_f results ($\times 10^5$) for unmanipulated adverse pressure gradient boundary layer

	Preston tube		Razor blade		Fence
ξ	(O)	(C)	(O)	(C)	(O≡C)
10	385	380	382	382	—
20	355	349	347	345	—
30	313	305	300	298	298
40	256	243	235	233	—
50	163	150	142	139	135
60	079	072	070	067	060
70	054	048	049	049	040
80	039	038	049	049	—
90	065	068	096	096	—

O = original data; C = corrected for effect of dp/dx and/or h^+ variations

the relationship derived by Frei and Thomann.[34] Comparative measurements were also made with a sublayer scale fence ($h_F^+<3.5$) and a razor blade ($h_{RB}^+<11$). The use of such techniques to measure skin friction has been discussed by Winter,[35] who provides an otherwise unpublished calibration for razor blades due to Gaudet. In zero pressure gradient, skin friction results evaluated using this relationship (which appears to be largely independent of detailed razor blade geometry as Gaudet has indicated in a private communication), and the established calibration curve for fences of Rechenberg,[36] were in good agreement with those obtained from the Preston tube by employing the calibrations of Head and Vasanta Ram (see Ref. 35). Independent measurements with a 25-mm-diameter floating-element drag balance (developed at Laval University and described in Ref. 4) resulted in C_f values consistently 5% lower (see Figure 5).

The adverse pressure gradient results are also presented in Table 1 and Figure 4. Those obtained with the razor blade have also been corrected for variations in h^+. Residual discrepancies between the three sets of data for the unmanipulated flow may be due to the influence of d^2p/dx^2. In studies of similar C_p distributions Hirt and Thomann[37] have found that corrections for history effects are required for d^+ or $h^+>3$. The negative error in the Preston tube measurements at $\xi=80$ relative to the razor blade ($h_{HB}^+=2$ at this station) is similar though larger than the one they found in this region of $d^2p/dx^2<0$, while both the Preston tube and razor blade show positive errors relative to the fence in the region where $d^2p/dx^2>0$. The latter effect is also evident in the results of a spanwise survey conducted at $\xi=30$ (see inset to Figure 4). This revealed variations of less than 4% over the central 30δ span of the tunnel in the absence of the manipulator. A similar variation was found when the manipulator was present except in the wake of the 4-mm-diameter threaded support legs and downstream of the tips of the plates, where C_f was increased by 28% or reduced by 7%, respectively.

The skin friction results for the manipulated layer confirmed earlier indications that even such a strong pressure gradient has little effect on the drag-reducing performance of the device. As a result, in the present case separation was induced. Up to that point the absolute and integrated C_f reduction was virtually the same as that recorded for a comparable tandem device with $l=1.9\delta$, $s=10\delta$, $h=0.75\delta$, $t=1$ mm operating at $Re_\theta=1500$ and $Re_1=25{,}000$ in a nominally zero pressure gradient, $\beta=0$ (see inset to Figure 7(a)). As a result the maximum $\%C_f$ reduction was increased, in fact in the present case reaching 100% since separation occurred, but delayed under the influence of the adverse pressure gradient. As indicated by Figure 6, this observation is consistent with results for weaker gradients. Similar findings have previously led to suggestions of larger reductions in the presence of an adverse gradient, but the present results show that any such conclusions based on $\%C_f$ reductions are misleading.

The promotion of separation by the manipulator would appear to limit the possibilities for attaining net drag reductions, but this was not evident in the flight tests. Bertelrud (private

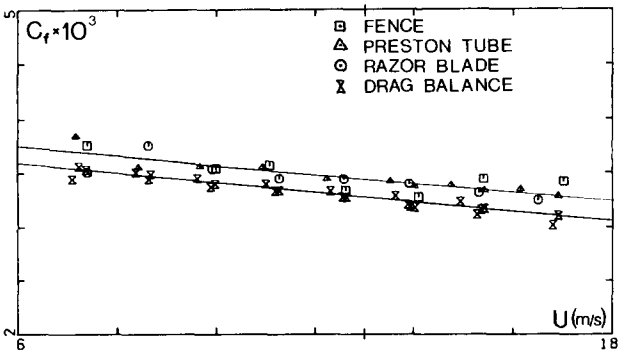

Figure 5 Comparison of zero-pressure gradient skin friction measurements obtained with various techniques

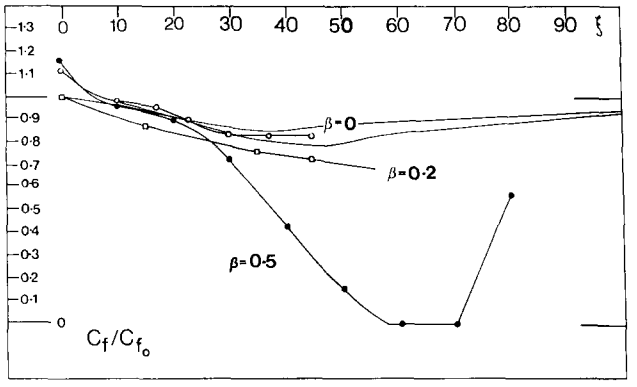

Figure 6 $\%C_f$ reductions recorded in zero and adverse pressure gradient tandem manipulated boundary layers: present results, —○—, $\beta=0$, —●—, $\beta_{max}=0.5$; —□—, $l=1.5\delta$, $s=5\delta$, $h=0.75\delta$, $t=1$ mm, $Re_\theta=3500$, $Re_t=38{,}000$, $\beta=0.2$;[2] ——, $l=1.2\delta$, $g=9.75\delta$, $h=0.63\delta$, $t=0.1$ mm, $Re_\theta=2950$, $Re_t=45{,}000$, $\beta=0$ and 0.2.[22]

communication) has suggested the explanation may be that the nonoptimal manipulators employed on the aircraft were mounted closer to the (wing) surface than ideal and therefore had their main effect well before separation was reached. Irrespective of this, van den Berg[38,39] has shown that it is the associated increase in shape factor H, rather than the magnitude of the attainable C_f reduction, which is more important for determining net drag performance under such conditions.

Turbulence modeling

The ASM was based on the Passable code developed at UMIST.[40] This makes use of a finite difference/finite volume forward marching scheme to solve the parabolic thin shear layer equations on a slightly nonorthogonal grid, which allows for flow development.

The closure scheme is based on modeled versions of the transport equations for the Reynolds stresses,

$$\frac{D\overline{u_iu_j}}{Dt}=T_{ij}+P_{ij}+\phi_{ij}-\tfrac{2}{3}\delta_{ij}\varepsilon \tag{1}$$

and, by analogy, the dissipation of turbulence energy,

$$\frac{D\varepsilon}{Dt}=T_\varepsilon+C_{\varepsilon_1}\left(\frac{\varepsilon}{k}\right)P_k-C_{\varepsilon_2}\left(\frac{\varepsilon^2}{k}\right) \tag{2}$$

where T_{ij}, P_{ij}, and ϕ_{ij} are identified as diffusion, production, and pressure-strain redistribution of the stresses, respectively. Summation over indices in Equation 1 leads to a similar expression for the transport of turbulence energy:

$$\frac{Dk}{Dt}=T_k+P_k+\varepsilon \tag{3}$$

while algebraic expressions for the Reynolds stresses are obtained by adopting the proposal of Rodi[41] that convective transport of the stresses occurs at the same rate as the transport of k, so

$$\frac{D\overline{u_iu_j}}{Dt}-T_{ij}=\frac{\overline{u_iu_j}}{k}\left(\frac{Dk}{Dt}-T_k\right)=\frac{\overline{u_iu_j}}{k}(P_k-\varepsilon) \tag{4}$$

and Equation 1 becomes

$$\frac{\overline{u_iu_j}}{k}(P_k-\varepsilon)=P_{ij}+\phi_{ij}-\tfrac{2}{3}\delta_{ij}\varepsilon \tag{5}$$

ϕ_{ij} is divided into three parts: return to isotropy ϕ_{ij1}, rapid pressure strain ϕ_{ij2}, and corresponding wall-reflection terms ϕ_{ijw_1} and ϕ_{ijw_2}. The following closure approximations are made:

$$T_k=C_k\frac{\partial}{\partial y}\left[\frac{k}{\varepsilon}\overline{v^2}\frac{\partial k}{\partial y}\right] \tag{6}$$

$$T_\varepsilon=C_\varepsilon\frac{\partial}{\partial y}\left[\frac{k}{\varepsilon}\overline{v^2}\frac{\partial \varepsilon}{\partial y}\right] \tag{7}$$

$$\phi_{ij1}=-C_1\frac{\varepsilon}{k}(\overline{u_iu_j}-\tfrac{2}{3}\delta_{ij}k) \tag{8}$$

$$\phi_{ij2}=-C_2(P_{ij}-\tfrac{2}{3}\delta_{ij}P_k) \tag{9}$$

$$\phi_{ijw_1}=-C_1'\frac{\varepsilon}{k}(\overline{u_n^2}\delta_{ij}-\tfrac{3}{2}\overline{u_nu_i}\delta_{nj}-\tfrac{3}{2}\overline{u_nu_j}\delta_{ni})f \tag{10}$$

$$\phi_{ijw}=-C_2'(\phi_{in_2}\delta_{ij}-\tfrac{3}{2}\phi_{ni_2}-\tfrac{3}{2}\phi_{nj_2}\delta_{ni})f \tag{11}$$

where $f=(k^{3/2}/C_w\varepsilon y)$ is a wall damping factor and n denotes the direction normal of the wall.

A two-layer wall treatment is employed in which the near-wall region is split into a viscous sublayer from $y=0$ to $y=y_v$, in which $\overline{uv}=0$, and an inertial sublayer stretching from y_v to the first grid point at y_p, in which $\overline{uv}$ increases linearly from an initial value equal to the wall shear stress τ. A velocity scale $\sqrt{k_v}$ is used in place of the friction velocity u_τ, and the value of y_v is set using a parameter R_v, where

$$R_v=y_vk_v^{1/2}\nu \tag{12}$$

The value of τ and hence the production and dissipation in the inertial sublayer are derived by assuming the standard log law:

$$U/u_\tau=A\log(yu_\tau/\nu)+B \tag{13}$$

For the present computations the log law constants were given the flat plate boundary layer values $A=5.62$ ($\equiv\kappa=0.41$) and $B=5.24$ required for consistency with independent measurements of u_τ. R_v was set to 18, which corresponded to a viscous sublayer thickness y_v of approximately 11 wall units. The values of the other constants were

$C_k=0.22$ $\quad C_\varepsilon=0.173$

$C_1=1.8$ $\quad C_2=0.6$

$C_1'=0.5$ $\quad C_2'=0.3$

$C_{\varepsilon_1}=1.44$ $\quad C_{\varepsilon_2}=1.92$

These are the same as those used for wake/boundary layer interactions[29,30] and, apart from C_k and C_ε, are almost identical to those employed by Launder *et al.*[28] for a very wide range of flows. $C_k=0.25$ and values of C_ε ranging from 0.15 to 0.18 have been adopted by several other workers. These were tested on the present flows, but none of the predicted quantities was altered by more than 1% by such changes.

For the adverse pressure gradient calculations the extra source terms due to streamwise gradients of the normal stresses were included in both the mean flow and turbulence equations. This involved the addition of a term

$$-C_{\varepsilon_3}\left(\frac{\varepsilon}{k}\right)\frac{dU}{dx}(\overline{u^2}-\overline{v^2}) \tag{14}$$

where C_{ε_3} is a function of strain rate, to the right side of Equation 2 in order to sensitize the dissipation to irrotational straining.[42] Such a modification requires the assumption[43] that the dissipative scales respond to the mean flow rates of strain in a similar manner as the larger energy-containing eddies because the two scales of motion are closely linked, and some justification for this, at least in the case of a wake, has recently

been provided by a pattern-recognition analysis of multiprobe hot-wire data.[44]

A conditional central/upwind differencing scheme is employed in the direction normal to the wall while the equations are implicit in x. A typical computation, with 40 points across the boundary layer (15 covering the manipulator wake) and 0.09δ steps in the stream direction (with six in-step iterations), solving for 16 stations up to 200δ downstream required 40 s of CPU time on the University IBM 3083/4, which is equivalent to 0.011 s/time step.

The model was applied in a purely predictive manner by starting the computations at the same station, 2.25δ behind the first plate of the tandem configuration, and using the same model constants and input profiles as for earlier zero pressure gradient calculations downstream of a single plate device. Preliminary results[21] have been corrected for flow divergence following the procedure suggested by Agoropoulos,[30] and similar computations for the unmanipulated layer have now been performed. The only constraint applied to the output presented in Figure 7(a),(b) was to require a close fit to the experimental data at the grid location nearest to the first measurement station behind the second element of the tandem. It can be seen that the ASM predictions are in remarkably good agreement with the experimental data, provided $C_{\varepsilon_3} = 2.5$ (Figure 7(a)), the figure recommended for such strong gradients,[45] rather than the value of 4.44 (Figure 7(b)) which has been suggested for weaker straining.[42] The predicted shape factor distribution has been plotted on Figure 8 and is seen to

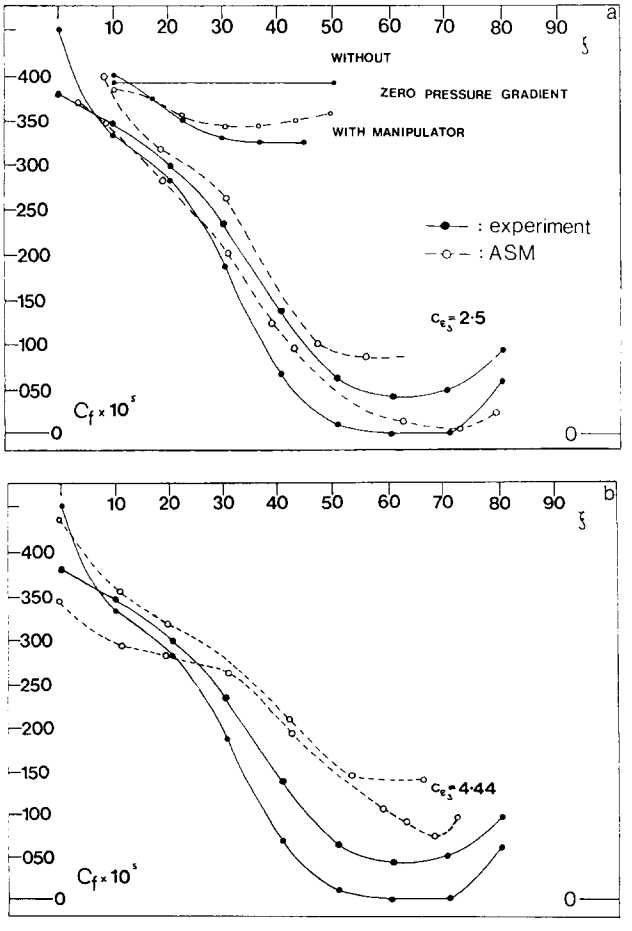

Figure 7 Skin friction distributions predicted with the ASM scheme using (*a*) $C_{\varepsilon_3}=2.5$ and (*b*) $C_{\varepsilon_3}=4.44$; compared with present experimental results

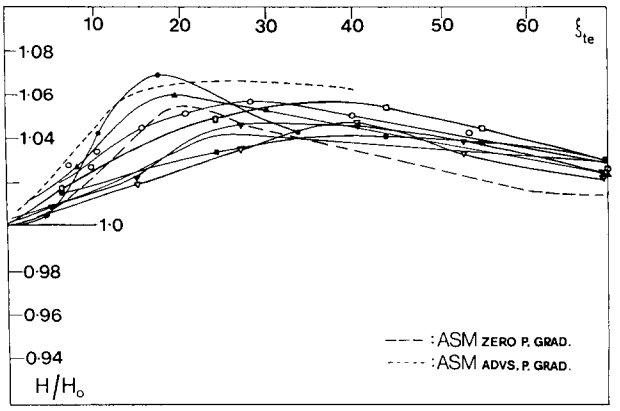

Figure 8 Shape factor distributions behind a range of manipulator devices under different flow conditions: single plates: ○, $l=0.8\delta$, $h=0.3\delta$, $t=0.12$, $Re_\theta=2500$, $Re_1=17{,}000$;[5] ●, $l=2.25\delta$, $h=0.5\delta$, $t=1$ mm, $Re_\theta=3000$, $Re_1=50{,}000$;[3] tandem plates: ▲, $l=1.1\delta$, $s=11\delta$, $h=0.5\delta$, $t=0.1$ mm, $Re_\theta=3200$, $Re_1=34{,}400$;[14] ▼, $l=1.25\delta$, $g=9\delta$, $h=0.8\delta$, $t=0.05$ mm, $Re_\theta=1500$, $Re_1=24{,}000$, ▽, + free stream turbulence;[23] ■, $l=0.95\delta$, $s=5.1\delta$, $h=0.75\delta$, $t=0.4$ mm, $Re_\theta=2400$, $Re_1=20{,}000$, □, $s=2.9\delta$;[4] tandem NACA 0009 aerofoils: —, $l=1.2\delta$, $s=5\delta$, $h=0.8\delta$, $Re_\theta=7400$, $Re_1=80{,}000$.[17]

be similar to those measured behind a range of devices, as well as that calculated with the ASM, in the absence of a pressure gradient. This finding seems to be consistent with the observation of a similar absolute C_f reduction in both cases, but points to a further restriction on net drag performance under such conditions since the increase in H (which mirrors the C_f reduction) in the manipulated flow is over and above the rise in H (in this case to 2.2) due to pressure gradient alone.

Concluding remarks

The results presented here indicate that even a severe adverse pressure gradient has remarkably little effect on the skin friction reduction behind a tandem manipulator and that the development of the manipulated layer can be adequately predicted by a turbulence model employing an algebraic Reynolds stress closure. However, two points should be noted: first, the present study has not addressed the effect of pressure gradient on the device itself, and, second, as pointed out by van den Berg,[39] even substantial C_f reductions will not be sufficient to ensure a net drag benefit when the increase in H is significant (indeed to achieve this it may even be necessary to increase C_f well before separation is approached).

As part of the same overall program of research into the possible use of manipulators in aerodynamic environments, a parallel series of experiments has been conducted by Roach and Brierley (see Refs. 7 and 23) at the Advanced Research Laboratory, Rolls-Royce plc, Derby, into the effect of free stream turbulence on manipulated flows. Together with the studies which have been made of manipulated rough (and Riblet) wall layers these suggest that such additional influences also have surprisingly little effect on manipulator performance. In each case it appears that the absolute magnitude of the C_f reduction (due to the manipulator) is approximately the same as that obtained with the same device in an undisturbed smooth wall layer (see Ref. 7 and Figure 9). This finding is contrary to prior expectations[7,12] that larger reductions might be possible in the presence of free stream turbulence, due to a beneficial blocking influence of manipulators wakes, and for the combination of Riblets and manipulators, with appropriate matching of parameters. However, the range of parameters so far considered

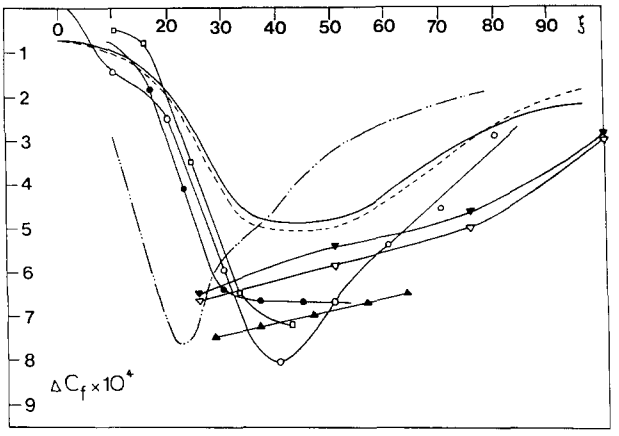

Figure 9 Comparison of absolute C_f reductions obtained in boundary layers subjected to tandem manipulation in combination with differing additional influences: present results, ○, $\beta=0$, ●, $\beta_{max}=0.5$; □, $\beta=0.2$, $l=1.5\delta$, $s=10\delta$, $h=0.75\delta$, $t=1$ mm, $Re_\theta=3500$, $Re_1=38{,}000$;[2] $\beta=0$: ▲, $l=1.1\delta$, $s=11\delta$, $h=0.5\delta$, $t=0.1$ mm, $Re_\theta=3200$, $Re_1=34{,}400$;[14] —, $l=1.25\delta$, $g=9\delta$, $h=0.8\delta$, $t=0.05$ mm, $Re_\theta=1500$, $Re_1=24{,}000$, ——, + free stream turbulence;[23] — ··, $l=1.2\delta$, $s=10\delta$, $h=0.8\delta$, $t=0.14$ mm, $Re_\theta=2900$, $Re_1=27{,}000$ + k-type roughness;[24] profiled plates: ▼, $l=1.0\delta$, $s=10\delta$, $h=0.8\delta$, $t=0.25$–0.05 mm, $Re_\theta=3000$, $Re_1=30{,}000$ + Riblets;[15,26] NACA 0009 aerofoils: ▽, $l=1.2\delta$, $s=10\delta$, $\alpha=0$, $h=0.8\delta$, $Re_\theta=7400$, $Re_1=80{,}000$.[17]

for all these extra effects is rather limited, in particular the free stream turbulence intensities ($<3\%$) and length scales ($<1.5\delta$) studied were small compared to those of interest in practice, and no attempt has so far been made to reoptimize devices under such conditions.

It is questionable whether the optimum parameters deduced from nominally zero-pressure gradient, undisturbed low-speed experiments are relevant to the practical application of an aerofoil section manipulator at flight speeds, particularly as there is already an indication[20] that larger α may then be beneficial because of the Katzmayr effect (see Ref. 1), and Anders (private communication) has suggested that a single element may be sufficient when its boundary layers are turbulent. The implication is that the emphasis of future research should be placed on parametric investigations at higher Mach and Reynolds numbers under controlled laboratory conditions, but such experiments are expensive, difficult to perform, and could usefully be complemented by computer predictions particularly for the effects of extra strain rates. The ASM model has recently been applied successfully to the weak free stream turbulence case studies by Roach and Brierley, and predictions for higher intensities and larger length scales than could be achieved in the experiments do indeed indicate a small improvement in manipulator performance.[46] The same parabolic code has recently been used to predict the effects of convex streamline curvature on a manipulated layer,[47] for which there is as yet no experimental information. The indication is that mild curvature ($\delta/R<0.05$) introduced behind the device would have little effect on the flow development while stronger curvature may delay the drag reduction.

However, to perform optimization studies of manipulator configurations, elliptic computations starting upstream of the devices are required. Some progress toward such parametric predictions has already been made by Tenaud, Coustols, and Cousteix.[32] Initial k-ε computations for the pressure field in the vicinity of a single thin plate device were in good agreement with their own experimental measurements plotted in Figure 3, and they were able to reproduce the general shape of the C_f distribution beneath such devices as measured with the razor blade technique by the present author.[12] Subsequent three- and five-equation differential stress transport model predictions indicated an optimum tandem plate separation in the region $s=10$–12δ ($g=7l$), close to that deduced from several experimental studies (see Refs. 12 and 21), and the predicted optimum height of $h=0.6\delta$ was also in good agreement with experimental findings. Remaining discrepancies between computations and experiments can largely be attributed to the adoption of a mixing length model for the device boundary layers and near-wall region. The extension to computer optimization of practical aerofoil manipulators will necessarily require a more sophisticated treatment of the unsteady flow around these devices. A patched zonal model may thus prove the best approach, in which case the present ASM scheme could be employed downstream of the device.

Acknowledgments

Thanks are due to Professor Hans Thomann for supplying the thesis of Hirt and Frei, whose work led to the development of the pressure gradient corrections for Preston tubes, and for helpful discussions concerning these; to Professor Brian Launder for making available the original ASM code through the course on 'numerical methods in heat and fluid flow' held at UMIST; to Dr. Demetri Agoropoulos for discussions on the application of this to wake/boundary layer flows; to Professor John Dickinson for the loan of the drag balance which he designed and built, and to his student Jean Lemay for assisting with the calibration of this during his period as a visiting researcher in Cambridge; to Dr. Paul Roach and Professor V. D. Nguyen for providing unpublished experimental data as private communications; and Rolls-Royce plc for supporting this work through University Research Project No. 8587.

References

1 Hefner, J. N., Weinstein, L. M., and Bushnell, D. M. Large-eddy breakup scheme for viscous drag reduction. *Prog. Astro. and Aero.*, 1979, **72**, 110–127

2 Bertelrud, A., Truong, T. V., and Avellan, F. Drag reduction in turbulence boundary layers using ribbons. AIAA Paper No. 1390, 1982

3 Mumford, J. C. and Savill, A. M. Parametric studies of flat plate, turbulence manipulators including direct drag results, and laser flow visualization. *Laminar Turbulent Boundary Layers ASME FED*, 1984, **11**, 41–51

4 Lemay, J., Provencal, D., Gourdeau, R., Nguyen, V. D., and Dickinson, J. More detailed measurements behind turbulence manipulators including tandem devices using servo controlled balances. AIAA Paper No. 0521, 1985

5 Coustols, E. and Cousteix, J. Reduction du frottement turbulent: moderateurs de turbulence. *La Recherche Aerospatiale*, 1986, **2**, 145–160

6 Savill, A. M. and Mumford J. C. Turbulent boundary layer manipulation by outer layer devices: skin friction and flow visualization results. *J. Fluid Mech.*, 1988, **191**, 389–418

7 Savill, A. M., Truong, T. V., and Rhyming, I. L. Turbulent drag reduction by passive means: a review and report on the first European drag reduction meeting. *EPFL Inst. Mach. Hydr. and Mech. Fluid. Rep.*, 1987, **T-87-3** and *J. de Mécanique*, 1988, **7**(4), 353–378

8 Corke, T. C., Nagib, H. M., and Guezennec, Y. G. A new view on the origin, role, and manipulation of large scales in turbulent boundary layers, NASA, CR 165861, 1982

9 Falco, R. E. New results, a review, and synthesis of the mechanisms of turbulence production in boundary layers and its modification. AIAA Paper No. 0377, 1983

10 Guezennec, Y. G. and Nagib, H. M. Documentation of the mechanisms leading to net drag reduction in manipulated boundary layers, AIAA Paper No. 0519, 1985

11 Narasimha, R. and Sreenivasan, K. R. The control of turbulent boundary layer flows. AIAA Paper No. 0517 and Dept. Aerosp. Eng. Rep. 1986 FM 4 Indian Inst. Sci., Bangalore, 1985

12 Savill, A. M. On the manner in which outer layer disturbances affect turbulent boundary layer skin friction, Advances in Turbulence. *Proc. European Turbulence Conf.*, Lyon, 1986, Springer-Verlag, 533–545

13 Wilkinson, S. P., Anders, J. B., Lazos, B. S., and Bushnell, D. M. Turbulent drag reduction research at NASA Langley—progress and plans. *Int. J. Heat and Fluid Flow*, 1988, **9**, 266–277

14 Plesniak, M. W. and Nagib, H. M. Net drag reduction in turbulent boundary layers resulting from optimized manipulation. AIAA Paper No. 0518, 1985

15 Anders, J. B., Hefner, J. N., and Bushnell, D. M. The performance of large-eddy breakup devices at post-transitional Reynolds numbers. AIAA Paper No. 0345, 1984

16 Poll, D. I. A. and Westland, P. G. A study of LEBU performance by direct total-force measurements. *Proc. Roy. Aero. Soc. Int. Conf. on Turbulent Drag Reduction by Passive Means*, London, 1, 1987, 33–44

17 Anders, J. B. and Watson, R. D. Airfoil large-eddy breakup devices for turbulent drag reduction. AIAA Paper No. 0520, 1985

18 Coustols, E., Cousteix, J., and Belanger, J. Drag reduction performances on riblet surfaces and through outer layer manipulators. *Proc. Roy. Aero. Soc. Int. Conf. on Turbulent Drag Reduction by Passive Means*, London, 2, 1987, 250–289

19 Bertelrud, A. Full scale experiments into the use of large-eddy break-up devices for drag reduction on aircraft. *AGARD Conf. Proc.*, 365, 1985, 1

20 Bertelrud, A. and Watson, R. D. Use of LEBU devices for drag reduction at flight conditions. *Proc. Roy. Aero. Soc. Int. Conf. on Turbulent Drag Reduction by Passive Means*, London, 1, 1987, 213–249

21 Savill, A. M. Turbulent boundary layer manipulation and modelling in zero and adverse pressure gradients. *Proc. IUTAM Conf. on Turbulence Management and Relaminarisation*, Bangalore, Springer-Verlag, 1987, 69–83

22 Veuve, M., Truong, T. V., and Rhyming, I. L. Detailed measurements downstream of a tandem manipulator in pressure gradients. *Proc. Roy. Aero. Soc. Int. Conf. on Turbulent Drag Reduction by Passive Means*, London, 1, 1987, 69–88

23 Roach, P. E. A new method of calculating the boundary layer characteristics downstream of manipulators, Part 1: Boundary layer integral parameters. Part 2: Skin friction and net drag reduction. *Proc. Roy. Aero. Soc. Int. Conf. on Turbulent Drag Reduction by Passive Means*, London, 1, 1987, 169–194 and 195–212

24 Bandyopadhyay, P. R. The performance of smooth-wall drag reducing devices in rough-wall boundary layers. AIAA Paper No. 0558, 1985 and *Expts. in Fluids*, 1986, **4**, 247–256

25 Pineau, F., Nguyen, V. D., Dickinson, J., and Belanger, J. Study of the flow over a rough surface with passive boundary layer manipulators and direct wall drag measurements. AIAA Paper No. 0357, 1987

26 Walsh, M. J. and Lindemann, A. M. Optimization and application of riblets for turbulent drag reduction. AIAA Paper No. 0347, 1984

27 Savill, A. M. Effects on turbulent boundary layer structure of longitudinal riblets alone and in combination with outer layer devices, Flow Viualisation IV. *Proc. 4th. Int. Symp. Flow Visualisation*, Paris, Hemisphere, 1986, 333–338

28 Launder, B. E., Leschziner, M. A., and Sindir, M. Computors summary report, Comparison of Computation with Experiment. *Proc. AFOSR-HTTM-Stanford Conf. on Complex Turbulent Flows*, 3, 1981, 1390–1407

29 Nemouchi, Z. Numerical computations of merging turbulent wakes and boundary layers. UMIST Mech. Eng. Dept. Rep., 1983, TFD/83/8

30 Agoropoulos, D. Interactions between wakes and boundary layers. Ph.D. thesis, University of Cambridge, 1986

31 Bandyopadhyay, P. R. and Watson, R. D. Pressure field due to drag reducing outer layer devices in turbulent boundary layers. *Expts. in Fluids*, 1987, **5**, 393–400

32 Tenaud, C., Coustols, E., and Cousteix, J. Modelling of turbulent boundary layers manipulated with thin outer layer devices. *Proc. Roy. Aero. Soc. Int. Conf. on Turbulent Drag Reduction by Passive Means*, London, 1, 1987, 144–168

33 Patel, V. C. Calibration of the Preston tube and limitations on its use in pressure gradients. *J. Fluid Mech.*, 1965, **23**, 185–208

34 Frei, D. and Thomann, H. Direct measurements of skin friction in a turbulent boundary layer with a strong adverse pressure gradient. *J. Fluid Mech.*, 1980, **101**, 79–95

35 Winter, K. G. An outline of the techniques available for the measurement of skin friction in turbulent boundary layers. *Prog. Aerospace Sci.*, 1977, **18**, 1–57

36 Rechenberg, I. The measurement of turbulent wall shear stress. ZFW 1963, 11, 11 and ARA Library Translation 1965, 11

37 Hirt, F. and Thomann, H. Measurement of wall shear-stress in turbulent boundary layers subjected to strong pressure gradients. *J. Fluid Mech.*, 1986, **171**, 547–562

38 van den Berg, B. Technical evaluators report on improvement of aerodynamic performance through boundary layer control and high lift systems. AGARD, 1985, CP 365, D-2, and NLR, 1986, MP 85016 U

39 van den Berg, B. Drag reduction potentials of turbulence manipulation in adverse pressure gradient flows. NLR, 1986, MP 86060 U

40 Leschziner, M. A. An introduction and guide to the computer code Passable. Dep. Mech. Eng. Rep., 1983, TFD/83/8

41 Rodi, W. A new algebraic relation for calculating the Reynolds stresses. *ZAMM*, 1976, **56**, T219–221

42 Hanjalic, K. and Launder, B. E. Sensitizing the dissipation equation to irrotational strains. *Trans ASME J. Fluids Eng.*, 1980, **102**, 34–40

43 Pope, S. B. An explanation of the turbulent round-jet/plane-jet anomaly. *AIAA J.*, 1978, **16**(3), 279–281

44 Ferre, J. A., Mumford, J. C., Savill, A. M., and Giralt, F. Three-dimensional large-eddy motions and fine-scale activity in a plane turbulent wake. *J. Fluid Mech.*, 1989, in press

45 Rodi, W. and Scheuerer, G. Scrutinising the k-ε model under adverse pressure gradient conditions. *Trans ASME J. Fluids Eng.*, 1986, **108**, 174–179

46 Savill, A. M. Algebraic and Reynolds stress modelling of manipulated boundary layers including effect of free-stream turbulence. *Proc. Roy. Aero. Soc. Int. Conf. on Turbulent Drag Reduction by Passive Means*, London, 1, 1987, 89–143

47 Savill, A. M. Structural refinements to Reynolds stress closures for plane, manipulated, and wake-boundary layers. To appear in *Proc. 3rd. Int. Symp. on Refined Modelling of Flows*, Tokyo, 1988, Universal Academy Press